Chiral Resolution

DOI: 10.1002/anie.201202081

Pasteurian Segregation on a Surface Imaged In Situ at the Molecular Level**

Hong Xu, Wojciech J. Saletra, Patrizia Iavicoli, Bernard Van Averbeke, Elke Ghijsens, Kunal S. Mali, Albertus P. H. J. Schenning, David Beljonne, Roberto Lazzaroni, David B. Amabilino,* and Steven De Feyter**

Dedicated to Professor Sir J. Fraser Stoddart on the occasion of his 70th birthday

The separation of enantiomers, which is an important step in the production of optically active chemicals for use in a variety of applications, is frequently performed using classical diastereomeric resolution, or Pasteurian resolution.[1–4] This crystallization process relies on the different solubility and crystallization propensity of the diastereomers formed by the enantiomers of a target racemate with a complementary chiral compound (the resolving agent), which forms a complex or a salt with it. The identification of the resolving agents that work for a given racemic mixture in this process relies on an empirical screening,[5] although some rationalization based on phase behavior or arguments based on supramolecular chemistry and molecular recognition can be invoked largely with hindsight.[6]

The study of Pasteurian resolution involving surfaces is interesting for a number of reasons, many of which arise from the reduced symmetry possibilities in this low-dimensional environment.[7] Unlike the situation in bulk crystals, spontaneous resolution is observed very frequently on crystalline surfaces wherein domains of opposite handedness arise.[8] Enantiomers often adsorb in mirror-image domains, though their separation and collection is a tremendous task. A demonstration of Pasteur's triage at the nanoscale was shown for mirror-image clusters using the tip of a scanning tunneling microscope (STM) as a nanoscale probe.[9]

Diastereomeric interactions on surfaces could be more powerful for practical separations. For instance, transfer of chirality from chemisorbed monolayers to bulk crystals has been used for the selective growth of crystals of one enantiomer in a racemic mixture in solution, which presumably involves diastereomeric interactions between the surface and the crystal nucleus,[11] while for similar cases conglomerates are formed.[12] Visualization of diastereomeric interactions on surfaces is rare. While the observation of diastereomeric interactions for the complex formed between phenylglycine and adenine was seen under ultrahigh vacuum conditions on a metal surface,[10] this process originates from the formation of chiral strips of the prochiral base followed by adhesion of the amino acid to it. It is therefore akin to a spontaneous resolution. There is no information regarding the formation of two-dimensional (2D) crystals of diastereomers in a dynamic system in solution. This observation could be very relevant to separation procedures involving the interaction of chiral molecules with surfaces.

Herein we demonstrate diastereoselective adsorption on an achiral surface by surface-mediated complex formation and the in situ visualization at the molecular level by employing STM at the liquid–solid interface (Scheme 1). As part of the process, a 2D crystal is formed, and as such it is a crystallization process, albeit more dynamic than the case of bulk crystals. Although only a small fraction of the molecules in solution are involved in 2D crystal formation because of the limited surface area of the substrate, we appeal to Pasteurian resolution, as the concept is identical in the sense that one diastereomeric complex is less soluble than the other and/or shows a pronounced affinity for adsorption onto

[*] Dr. H. Xu, E. Ghijsens, Dr. K. S. Mali, Prof. S. De Feyter
Division of Molecular Imaging and Photonics, Department of Chemistry, KU Leuven—University of Leuven, Celestijnenlaan 200 F, B-3001, Leuven (Belgium)
E-mail: steven.defeyter@chem.kuleuven.be

W. J. Saletra, Dr. P. Iavicoli, Prof. D. B. Amabilino
Institut de Ciència de Materials de Barcelona (ICMAB-CSIC), Campus Universitari de Bellaterra, 08193 Cerdanyola del Vallès (Catalonia, Spain)
E-mail: amabilino@icmab.es

Dr. B. Van Averbeke, Dr. D. Beljonne, Prof. R. Lazzaroni
Service de Chimie des Matériaux Nouveaux, Université de Mons (UMONS), Place du Parc 20, 7000 Mons (Belgium)
E-mail: roberto.lazzaroni@umons.ac.be

Prof. A. P. H. J. Schenning
Laboratory of Functional Organic Materials and Devices (SFD), Eindhoven University of Technology, P.O. Box 513, 5600 MB Eindhoven (the Netherlands)

[**] This work was supported by the European Commission Seventh Framework Programme under grant agreement no. NMP4-SL-2008-214340, project RESOLVE, KU Leuven (GOA), Funding for Scientific Research—Flanders (F.W.O.), IWT, the Belgian Federal Science Policy Office through IAP 7/05, the Belgian National Fund for Scientific Research (FNRS-FRFC), the OPTI2MAT "Pole d'Excellence" Programme of Region Wallonne, the Spanish MINECO (Project CTQ2010-16339), and DGR, Catalonia (Project 2009 SGR 158). W.J.S. thanks the CSIC for a JAE predoctoral grant co-financed by the FSE. D.B. is FNRS research director. We thank Meir Lahav for useful comments.

Supporting information for this article is available on the WWW under http://dx.doi.org/10.1002/anie.201202081.

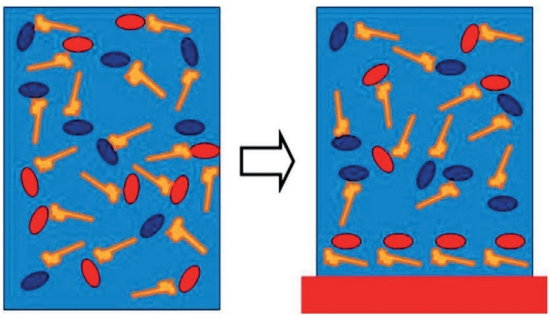

Scheme 1. A cartoon depicting diastereoselective crystallization at the liquid–solid interface. The hammer-like features symbolize the enantiopure resolving agents. The red and blue ovals represent the enantiomers of the racemate to be resolved.

the achiral substrate and is therefore preferentially taken up in the surface adsorbed crystal, leaving the other diastereomer in solution. We used STM, supported by molecular modeling,[13] to visualize the diastereoselective adsorption process and the chiral resolution at the nanoscale. Various phenomena related to surface chirality have been revealed with the technique,[8,14] but to the best of our knowledge, none of them deal with diastereomeric resolution by surface-mediated diastereomeric complex formation in solution.

An alkylated resorcinol derivative (**1**) with a lactate moiety, which is the source of chirality, was selected as the potential resolving agent, as the compound itself displays spontaneous resolution on highly oriented pyrolytic graphite (HOPG).[15] The octadecyloxy chains favor monolayer formation by physisorption through C–H···π interactions with HOPG and van der Waals interactions between those chains. 1-Phenyloctane was used as the solvent, as it fulfills technical requirements for STM at the liquid–solid interface. *Rac*-1,2-diaminocyclohexane (a 1:1 mixture of (*R*,*R*)- and (*S*,*S*)-**2**) served as the racemate because the amine groups can interact with the hydrogen-bond donors in the acid group of the resolving agent. The enantiomers of **1** form enantiomorphous monolayers on HOPG when adsorbed from 1-phenyloctane.[15] The individual resorcinol residues can be identified by STM, showing that nearest-neighbor molecules of different rows form dimers which are organized in lamellae over large areas up to several square micrometers. The alkyl chains are fully extended on the surface, running nearly perpendicular to the row axis, and are interdigitated with those of adjacent rows. The width of a row (D1) is about 3.7 nm (Figure 1 b). Molecule **2** does not self-assemble into a monolayer that is stable enough to withstand STM imaging.

Upon premixing like enantiomers of **1** and **2** in solution and deposition on the substrate, a new packing pattern is observed. Figure 1 c,d show typical STM images of such monolayers formed by [(*R*)-**1** + (*R*,*R*)-**2**] and [(*S*)-**1** + (*S*,*S*)-**2**] respectively, at a solution ratio of 2:1. The width of the molecular rows (D2) is about 5.3 nm, which is much larger than that of enantiopure **1** (D1 = 3.7 nm). Rows consist of abutted tail-to-tail molecules of **1**. The alkyl chains are not interdigitated, but this feature explains only in part the increased width of the rows. Based on the orientation and packing of the alkyl chains, the distance between resorcinol

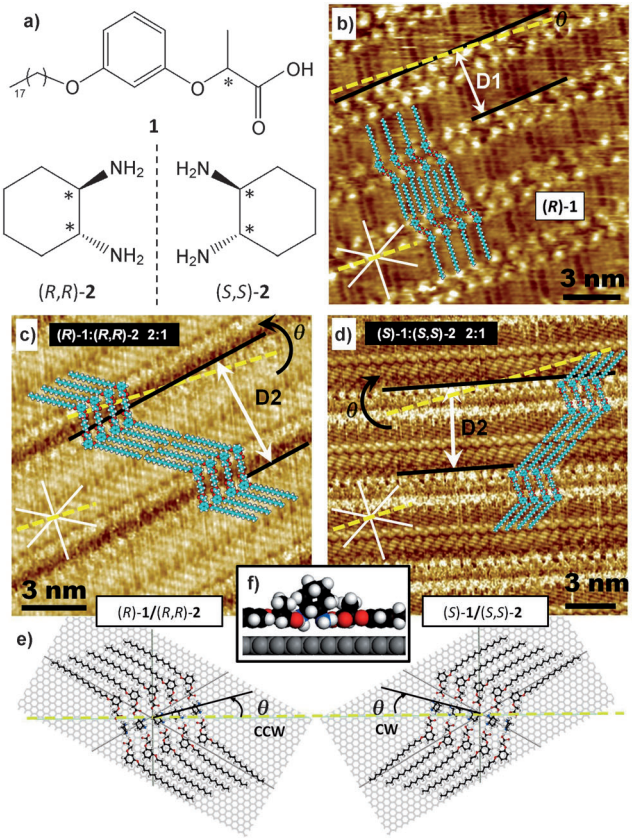

Figure 1. a) Chemical structures of the chiral resorcinol derivative **1** and 1,2-diaminocyclohexane **2**. ⋆ indicates the location of a stereogenic center. STM images of monolayers at the 1-phenyloctane–HOPG interface formed by b) (*R*)-**1** (I_{set} = 0.70 nA; V_{set} = 0.50 V) and c), d) upon premixing **1** and **2** at a 2:1 ratio. c) (*R*)-**1**: (*R*,*R*)-**2** (2:1) (I_{set} = 0.25 nA; V_{set} = 1.00 V), d) (*S*)-**1**: (*S*,*S*)-**2** (2:1) (I_{set} = 0.20 nA; V_{set} = 1.00 V). The solution composition is shown in a black text box, whereas the domain composition is given in a white text box. White solid lines indicate the main symmetry axes of graphite. Yellow dashed lines indicate the selected graphite reference axis running perpendicular to one of the main symmetry axes. Black solid lines indicate the direction of molecular rows. θ is the angle between the row axis and the HOPG reference axis. Double-headed arrows show the width (*D*) of the rows. Models of resorcinol and diamine molecules are superimposed on the STM image. e) Molecular model of the z-shaped (*R*)-**1**/(*R*,*R*)-**2** self-assembled structure on graphite obtained by molecular mechanics simulations. The model at the right is the s-shaped (*S*)-**1**/(*S*,*S*)-**2** structure which is obtained by reflection. The yellow dashed line is the graphite reference axis. f) Snapshot of representative structure (side view) of the core of the (*R*)-**1**/(*R*,*R*)-**2** assembly (N blue, O red).

groups of adjacent molecules along the propagation directions of the rows is only about 0.7 nm. This distance is less than that for the enantiopure **1** alone (ca. 1.0 nm). When the molecules of **2** can be identified in the STM images, they indicate the formation of a **1**-**2**-**1** complex, the diaminocyclohexane being located between two lactate groups (Figure 1 e). The location of the diaminocyclohexane groups often appears fuzzy in the STM images. These streaky features are attributed to the tip knocking the molecular segments standing above the plane of the alkyl chains in the monolayer. This interpretation is supported by molecular modeling showing

that the 1,2-diaminocyclohexane units can protrude above the alkylated resorcinol derivative (Figure 1 f).

In contrast to the enantiopure layers of the pure acids where the alkyl chains are oriented quasi-perpendicular to the lamellar direction, the 2D chirality of the monolayers of the **1**-**2**-**1** complex can clearly be determined by the orientation of the alkyl chains with respect to the row axis. For the complex of (*R*)-**1** with (*R*,*R*)-**2** the alkyl chains are rotated counterclockwise (CCW) with respect to the normal of the row axis and clockwise (CW) in the (*S*)-**1** and (*S*,*S*)-**2** case (Figure 1). Furthermore, the monolayer chirality is also established by the relative orientation of the row axis with respect to the graphite lattice. The angle θ between the row axis and the HOPG reference axes $\langle -1\,1\,0\,0\rangle$ is $-10\pm2°$ in monolayers of (*R*)-**1**/(*R*,*R*)-**2** (Figure 1 c,e) and $+12\pm3°$ for (*S*)-**1**/(*S*,*S*)-**2** (Figure 1 d, e). The angles for the pure acids are $-4\pm2°$ ((*R*)-**1**) and $+5\pm3°$ ((*S*)-**1**), respectively (Supporting Information, Table S3; Figure 1 b for (*R*)-**1**).

Compounds that form diastereomeric complexes upon premixing do the same upon sequential addition. In such an experiment, domains of (*R*)-**1** disappear in time after addition of a droplet of a solution of (*R*,*R*)-**2** in 1-phenyloctane, as they are gradually replaced by domains composed of the complex (*R*)-**1**/(*R*,*R*)-**2** (Supporting Information, Figure S6). This dynamics in the monolayers can be followed by STM in real time revealing that the replacement of the surface-bound acid with the complex is relatively fast (for the present case after 5 min).

Unlike the combinations of acids and amine described above, mixtures of unlike enantiomers (*R*)-**1** and (*S*,*S*)-**2**, or (*S*)-**1** and (*R*,*R*)-**2** at the ratio of 2:1 do not lead to complex formation. Only monolayers of the acid are observed, with molecular packing and chiral expression identical to those of the enantiopure acids alone. Only at higher mole ratios (1:5 or 1:10) in case of the (*R*)-**1** and (*S*,*S*)-**2** system, a small number of domains suggesting complex formation were observed. (Supporting Information, Figure S8). Whatever the experimental conditions, (*S*)-**1**/(*R*,*R*)-**2** complexes were never observed. Therefore, we can conclude that the formation of surface-supported diastereomeric complexes (*R*)-**1**/(*R*,*R*)-**2** and (*S*)-**1**/(*S*,*S*)-**2** is more favorable than (*R*)-**1**/(*S*,*S*)-**2** and (*S*)-**1**/(*R*,*R*)-**2**. This result is crucial in view of the targeted diastereoselective adsorption experiments that aim at selectively adsorbing one of the diamine derivatives from a racemate with the help of the resolving acid. Furthermore, it is important to note that in the unlikely event that complexes are formed between unlike enantiomers of **1** and **2** on surface, they can be distinguished from the more stable complexes between alike enantiomers by the orientation of the alkyl chains.

To gain insight into the structure and energy characteristics of the absorbed diastereomeric complexes, a joint molecular mechanics/molecular dynamics (MM/MD) approach was used to model self-assembled monolayers of (*R*)-**1** interacting with either (*R*,*R*)- or (*S*,*S*)-**2** (in a 2:1 ratio) on a graphite substrate. Good agreement is found between the experimental and theoretical values for the lattice parameters (Supporting Information, Table S1), which validates the models proposed for the supramolecular organization of the chiral molecules on graphite. Furthermore, the calculations shed light on the arrangement of the molecules of **2** in the diastereomeric combinations considered ((*R*)-**1**/(*R*,*R*)-**2** versus (*R*)-**1**/(*S*,*S*)-**2**), which cannot be directly assessed from the STM images. This is key information, as the interactions between **1** and **2** entail the stereoselective adsorption of one diastereomer. While the (*R*,*R*)-**2** molecules can insert well in between two adjacent rows of (*R*)-**1** forming an ordered hydrogen-bond array, this is not the case for the (*S*,*S*)-**2** molecules, which, owing to the spatial arrangement of their amino groups, are only amenable to hydrogen bonding with one row of (*R*)-**1** (Supporting Information, Figure S9). Note that the majority of the hydrogen bonds are formed between the COOH group of resorcinol as the acceptor and the NH_2 groups of the diamine as the donor (Supporting Information, Figure S9). An energy analysis (Supporting Information, Table S2) suggests that the formation of a 2:1 complex of (*R*)-**1** with (*R*,*R*)-**2** is more stable by about 1.8 kT (4.5 kJ mol^{-1}) at 300 K than its (*R*)-**1**/(*S*,*S*)-**2** counterpart. The data also clearly point to the fact that the stabilizing

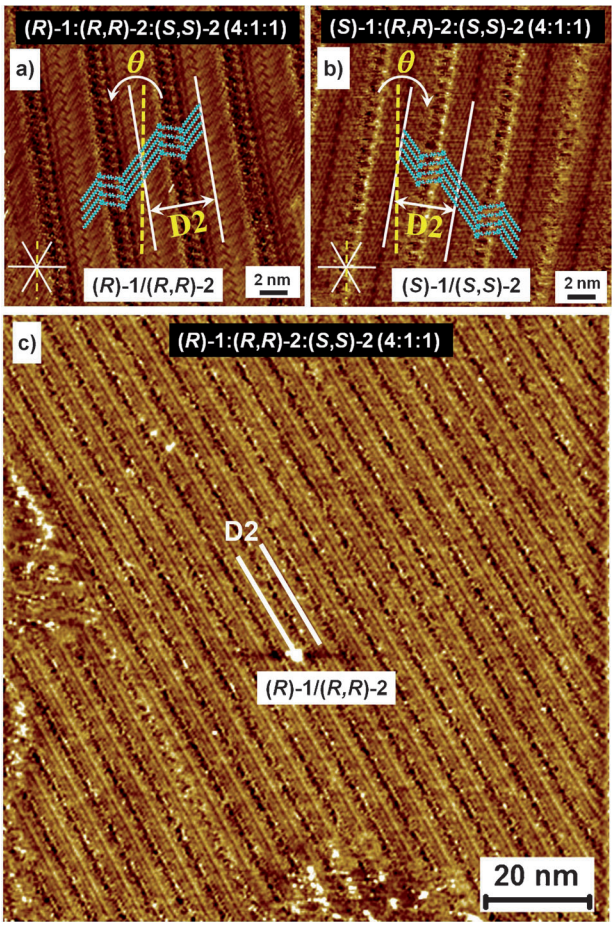

Figure 2. STM images of monolayers formed upon premixing one enantiomer of **1**, and the racemate of **2** at the 1-phenyloctane–HOPG interface. Molecular models are superimposed on top of the STM images. a) (*R*)-**1**:(*R*,*R*)-**2**:(*S*,*S*)-**2** (4:1:1) ($I_{set}=0.30$ nA; $V_{set}=1.00$ V), b) (*S*)-**1** : (*R*,*R*)-**2**: (*S*,*S*)-**2** (4:1:1) ($I_{set}=0.30$ nA; $V_{set}=1.00$ V). c) Large-scale STM image of (*R*)-**1**/(*R*,*R*)-**2** formed from a solution of (*R*)-**1**:(*R*,*R*)-**2**:(*S*,*S*)-**2** (4:1:1) ($I_{set}=0.15$ nA; $V_{set}=0.85$ V).

contributions favoring the (*R*)-**1**/(*R*,*R*)-**2** assembly arise from electrostatic interactions and hydrogen bond terms, in other words from interactions taking place between the polar head groups of **1** and **2**.

To explore the ability of **1** to selectively co-adsorb one of the enantiomers of **2**, (*R*)-**1** or (*S*)-**1** were premixed with equal amounts of (*R*,*R*)-**2** and (*S*,*S*)-**2**, that is, *rac*-**2**. Adding *rac*-**2** to (*R*)-**1** leads to the anticipated two-component pattern consisting of (*R*)-**1**/(*R*,*R*)-**2** for a solution composition with a ratio ranging from 4:1:1 up to 1:10:10 (Figure 2 and the Supporting Information). The same holds true for (*S*)-**1** and *rac*-**2**, where (*S*)-**1**/(*S*,*S*)-**2** is observed. Most importantly, monolayer patterns characteristic for diastereomeric complex formation involving (*R*)-**1** and (*S*,*S*)-**2** [(*R*)-**1**/(*S*,*S*)-**2**] or (*S*)-**1** and (*R*,*R*)-**2** [(*S*)-**1**/(*R*,*R*)-**2**] were never observed. These results clearly show the capacity of the acid to selectively co-adsorb one of the enantiomers of the amine by diastereoselective adsorption. Thus, acid resolves amine at the surface.[16]

In summary, Pasteurian diastereomeric segregation has been achieved at the liquid–solid interface in an equilibrating system thanks to the appropriate design of a resolving agent capable of interacting with the surface. Upon combining a resolving agent with good affinity for the substrate with the racemic mixture of a compound with lower affinity for the substrate, one of the latter enantiomers is exclusively adsorbed as a diastereomeric complex on the achiral graphite substrate; the other enantiomer is left in solution. This discovery bodes well for the development of studies of diastereoselective phenomena at interfaces to deepen understanding of interfacial diastereomer complexes and their possible exploitation. The observation of this diastereoselectivity at an interface also opens the opportunity for the study of more complex resolution phenomena under similar conditions in dynamic systems. The results presented show the potential for STM to probe stereochemical processes usually associated with much larger scales, giving submolecular-level information.

Experimental Section

All of the STM experiments were performed at room temperature using a PicoSPM (Agilent) machine operating in constant-current mode. Mechanically cut tips were used in the measurements (Pt/Ir wire 80%/20%, diameter 0.25 mm). The compounds under investigation were dissolved in 1-phenyloctane (Aldrich, 98%). Compound **1** was synthesized according to the reported procedure,[15] whereas **2** was obtained from Acros (99%). The overall concentration of **1** in the solution is always 7.6×10^{-3} M while the concentration of **2** is varied from sample to sample depending on the molar ratio of **1** and **2**. A drop of the solution was applied on a freshly cleaved surface of highly oriented pyrolytic graphite (HOPG) (grade ZYB, Advanced Ceramics Inc., Cleveland, OH). Then, the STM tip was immersed into the solution and scanned: a bright (dark) contrast refers to a high (low) height. The bias voltage was applied to the sample in such a way that, at negative bias voltage, electrons tunnel from the sample to the tip.

MD simulations were carried out with the Dreiding force field in the NVT ensemble at 298 K for 1 ns. The assemblies were built by applying periodic boundary conditions on a unit cell containing a frozen graphite bilayer and two rows of ten (*R*)-**1** resorcinol molecules, separated by a central row of ten (*R*,*R*)- or (*S*,*S*)-**2** diamine molecules.

Information on materials, additional STM images, structural analysis, and molecular modeling is provided in the Supporting Information.

Received: March 15, 2012
Revised: July 16, 2012
Published online: October 24, 2012

Keywords: chirality · diastereomers · resolution · scanning probe microscopy · selectivity

[1] L. Pasteur, *C. R. Hebd. Seances Acad. Sci.* **1853**, *37*, 162–166.
[2] L. Pasteur, *Ann. Chim.* **1853**, *38*, 437–483.
[3] J. Jacques, A. Collet, S. H. Wilen, *Enantiomers, racemates and resolutions*, Krieger Publishing Company, Malabar, FL, **1994**.
[4] a) E. Fogassy, M. Nógrádi, D. Kozma, G. Egri, E. Pálovics, V. Kiss, *Org. Biomol. Chem.* **2006**, *4*, 3011–3030; b) F. Faigl, E. Fogassy, M. Nógrádi, E. Pálovics, J. Schindler, *Tetrahedron: Asymmetry* **2008**, *19*, 519–536.
[5] *CRC Handbook of Optical Resolutions via Diastereomeric Salt Formation* (Ed.: D. Kozma), CRC Press, New York, **2002**.
[6] G. Coquerel, D. B. Amabilino in *Chirality at the Nanoscale* (Ed.: D. B. Amabilino), Wiley-VCH, Weinheim, **2009**, pp. 305–348.
[7] a) I. Weissbuch, I. Kuzmenko, M. Berfeld, L. Leiserowitz, M. Lahav, *J. Phys. Org. Chem.* **2000**, *13*, 426–434; b) I. Weissbuch, M. Lahav, *Chem. Rev.* **2011**, *111*, 3236–3267.
[8] a) F. Stevens, D. J. Dyer, D. M. Walba, *Angew. Chem.* **1996**, *108*, 955–957; *Angew. Chem. Int. Ed. Engl.* **1996**, *35*, 900–901; b) F. Stevens, N. A. Clark, D. C. Parks, *Acc. Chem. Res.* **1996**, *29*, 591–597; c) S. De Feyter, P. C. M. Grim, M. Rücker, P. Vanoppen, C. Meiners, M. Sieffert, S. Valiyaveettil, K. Müllen, F. C. De Schryver, *Angew. Chem.* **1998**, *110*, 1281–1284; *Angew. Chem. Int. Ed.* **1998**, *37*, 1223–1226; d) M. Ortega Lorenzo, C. J. Baddeley, C. Muryn, R. Raval, *Nature* **2000**, *404*, 376–379; e) V. Humblot, S. M. Barlow, R. Raval, *Prog. Surf. Sci.* **2004**, *76*, 1–19; f) S. Romer, B. Behzadi, R. Fasel, K.-H. Ernst, *Chem. Eur. J.* **2005**, *11*, 4149–4154; g) L. Pérez-García, D. B. Amabilino, *Chem. Soc. Rev.* **2007**, *36*, 941–967; h) M. Lingenfelder, G. Tomba, G. Costantini, L. C. Ciacchi, A. De Vita, K. Kern, *Angew. Chem.* **2007**, *119*, 4576–4579; *Angew. Chem. Int. Ed.* **2007**, *46*, 4492–4495; i) K. E. Plass, A. L. Grzesiak, A. J. Matzger, *Acc. Chem. Res.* **2007**, *40*, 287–293; j) N. Katsonis, E. Lacaze, B. L. Feringa, *J. Mater. Chem.* **2008**, *18*, 2065–2073; k) I. Paci, *J. Phys. Chem. C* **2010**, *114*, 19425–19432; l) A. Robin, P. Iavicoli, K. Wurst, M. S. Dyer, S. Haq, D. B. Amabilino, R. Raval, *Cryst. Growth Des.* **2010**, *10*, 4516–4525; m) E. V. Iski, H. L. Tierney, A. D. Jewell, E. C. H. Sykes, *Chem. Eur. J.* **2011**, *17*, 7205–7212; n) M. M. Knudsen, N. Kalashnyk, F. Masini, J. R. Cramer, E. Lægsgaard, F. Besenbacher, T. R. Linderoth, K. V. Gothelf, *J. Am. Chem. Soc.* **2011**, *133*, 4896–4905; o) M. Stöhr, S. Boz, M. Schär, M.-T. Nguyen, C. A. Pignedoli, D. Passerone, W. B. Schweizer, C. Thilgen, T. A. Jung, F. Diederich, *Angew. Chem.* **2011**, *123*, 10158–10162; *Angew. Chem. Int. Ed.* **2011**, *50*, 9982–9986.
[9] M. Böhringer, K. Morgenstern, W. D. Schneider, R. Berndt, *Angew. Chem.* **1999**, *111*, 832–834; *Angew. Chem. Int. Ed.* **1999**, *38*, 821–823.
[10] Q. Chen, N. V. Richardson, *Nat. Mater.* **2003**, *2*, 324–328.
[11] Y. Mastai, *Chem. Soc. Rev.* **2009**, *38*, 772–780.
[12] M. Ejgenberg, Y. Mastai, *Chem. Commun.* **2011**, *47*, 12161–12163.
[13] M. Linares, A. Minoia, P. Brocorens, D. Beljonne, R. Lazzaroni, *Chem. Soc. Rev.* **2009**, *38*, 806–816.

[14] a) T. E. Jones, C. J. Baddeley, *Surf. Sci.* **2002**, *519*, 237 – 249; b) Y. Wei, K. Kannappan, G. W. Flynn, M. B. Zimmt, *J. Am. Chem. Soc.* **2004**, *126*, 5318 – 5322; c) K. H. Ernst, *Top. Curr. Chem.* **2006**, *265*, 209 – 252; d) A. Kühnle, T. R. Linderoth, F. Besenbacher, *J. Am. Chem. Soc.* **2006**, *128*, 1076 – 1077; e) N. Liu, S. Haq, G. R. Darling, R. Raval, *Angew. Chem.* **2007**, *119*, 7757 – 7760; *Angew. Chem. Int. Ed.* **2007**, *46*, 7613 – 7616; f) W. Xiao, X. Feng, P. Ruffieux, O. Gröning, K. Müllen, R. Fasel, *J. Am. Chem. Soc.* **2008**, *130*, 8910 – 8912; g) U. Schlickum, R. Decker, F. Klappenberger, G. Zoppellaro, S. Klyatskaya, W. Auwärter, S. Neppl, K. Kern, H. Brune, M. Ruben, J. V. Barth, *J. Am. Chem. Soc.* **2008**, *130*, 11778 – 11782; h) S. Haq, N. Liu, V. Humblot, A. P. J. Jansen, R. Raval, *Nat. Chem.* **2009**, *1*, 409 – 414; i) J. A. A. W. Elemans, I. De Cat, H. Xu, S. De Feyter, *Chem. Soc. Rev.* **2009**, *38*, 722 – 736; j) R. Raval, *Chem. Soc. Rev.* **2009**, *38*, 707 – 721; k) L. Burkholder, D. Stacchiola, J. A. Boscoboinik, W. T. Tysoe, *J. Phys. Chem. C* **2009**, *113*, 13877 – 13885; l) P. Iavicoli, H. Xu, L. N. Feldborg, M. Linares, M. Paradinas, S. Stafström, C. Ocal, B. Nieto-Ortega, J. Casado, J. T. López Navarrete, R. Lazzaroni, S. De Feyter, D. B. Amabilino, *J. Am. Chem. Soc.* **2010**, *132*, 9350 – 9362; m) M. E. Cañas-Ventura, K. Aït-Mansour, P. Ruffieux, R. Rieger, K. Müllen, H. Brune, R. Fasel, *ACS NANO* **2011**, *5*, 457 – 469; n) F. Masini, N. Kalashnyk, M. M. Knudsen, J. R. Cramer, E. Lægsgaard, F. Besenbacher, K. V. Gothelf, T. R. Linderoth, *J. Am. Chem. Soc.* **2011**, *133*, 13910 – 13913; o) J. Liu, T. Chen, X. Deng, D. Wang, J. Pei, L. J. Wan, *J. Am. Chem. Soc.* **2011**, *133*, 21010 – 21015; p) K. Tahara, H. Yamaga, E. Ghijsens, K. Inukai, J. Adisoejoso, M. O. Blunt, S. De Feyter, Y. Tobe, *Nat. Chem.* **2011**, *3*, 714 – 719; q) V. Demers-Carpentier, G. Goubert, F. Masini, R. Lafleur-Lambert, Y. Dong, S. Lavoie, G. Mahieu, J. Boukouvalas, H. L. Gao, A. M. H. Rasmussen, L. Ferrighi, Y. X. Pan, B. Hammer, P. H. McBreen, *Science* **2011**, *334*, 776 – 780; r) I. De Cat, Z. Guo, S. J. George, E. W. Meijer, A. P. H. J. Schenning, S. De Feyter, *J. Am. Chem. Soc.* **2012**, *134*, 3171 – 3177.

[15] P. Iavicoli, H. Xu, T. Keszthelyi, J. Telegdi, K. Wurst, B. Van Averbeke, W. J. Saletra, A. Minoia, D. Beljonne, R. Lazzaroni, S. De Feyter, D. B. Amabilino, *Chirality* **2012**, *24*, 155 – 166.

[16] Both enantiomers of each component interact with each other in $CDCl_3$ (1-phenyloctane is not a suitable solvent for these NMR experiments), so both the complexes exist in solution. The diastereoselectivity occurs upon adsorption.

